Peptide-Functionalized Oxime Hydrogels with Tunable Mechanical Properties and Gelation Behavior

ARTICLE *in* BIOMACROMOLECULES · SEPTEMBER 2013

Impact Factor: 5.75 · DOI: 10.1021/bm401133r · Source: PubMed

Article

pubs.acs.org/Biomac

Peptide-Functionalized Oxime Hydrogels with Tunable Mechanical Properties and Gelation Behavior

Fei Lin,[†] Jiayi Yu,[†] Wen Tang,[†] Jukuan Zheng,[†] Adrian Defante,[†] Kai Guo,[†] Chrys Wesdemiotis,[†,‡] and Matthew L. Becker*[,†,§]

Departments of [†]Polymer Science and [‡]Chemistry, The University of Akron, Akron, Ohio 44325, United States

[§]Center for Biomaterials in Medicine, Austen Bioinnovation Institute in Akron, Akron, Ohio 44308, United States

Supporting Information

ABSTRACT: We demonstrate the formation of polyethylene glycol (PEG) based hydrogels via oxime ligation and the photoinitiated thiol−ene 3D patterning of peptides within the hydrogel matrix postgelation. The gelation process and final mechanical strength of the hydrogels can be tuned using pH and the catalyst concentration. The time scale to reach the gel point and complete gelation can be shortened from hours to seconds using both pH and aniline catalyst, which facilitates the tuning of the storage modulus from 0.3 to over 15 kPa. Azide- and alkene-functionalized hydrogels were also synthesized, and we have shown the post gelation "click"-type Huisgen 1,3 cycloaddition and thiolene-based radical reactions for spatially defined peptide incorporation. These materials are the initial demonstration for translationally relevant hydrogel materials that possess tunable mechanical regimes attractive to soft tissue engineering and possess atom neutral chemistries attractive for post gelation patterning in the presence or absence of cells.

INTRODUCTION

Hydrogels represent a diverse class of polymeric networks that absorb significant amount of water without dissolution. Hydrogels are utilized widely in tissue engineering, drug and protein delivery, cell culture, and sensors due to their unique and highly tunable chemical, mechanical, and transport properties.[1−5] In biomedical applications, cells and tissues sense and respond to the rigidity of their microenvironments and are able to alter their migration, signaling, differentiation, and proliferation responses.[6−9] It is essential that hydrogels targeted to tissue engineering scaffolds match the mechanical properties of target tissues.[10,11] Therefore, the biomaterials community continually searches for new hydrogel materials where the mechanical properties and network formation times are highly tunable.[12−16]

Polyethylene glycol (PEG) based hydrogels are utilized frequently due to the lack of cytotoxicity, unique hydration properties, and ease of end group modification for cross-linking or network formation.[17−19] Although much success can be attributed to the fabrication of PEG hydrogels via conventional photoinitiated free-radical chain polymerization,[20−22] trends have been moving toward building hydrogels through more robust, selective, efficient, and tunable chemical reactions.[23,24] Various types of "click" chemistry strategies have been employed to prepare hydrogels, including Michael-addition,[25−27] thiol−ene radical addition,[28,29] tetrazine−norbornene addition,[30,31] tetrazine−alkene photo click reaction,[32] copper-(I)-catalyzed alkyne−azide cycloaddition (CuAAC),[33−36] or metal-free strain-promoted alkyne−azide cycloadditions (SPAAC),[37−39] and so on. While these strategies are used as cross-linking methodologies, there have been increasing interests to combine several "click" reactions into one system to create more complex and biologically patterned microenvironments. Anseth and co-workers demonstrated that photoinitiated thiol−ene chemistry can be employed to spatiotemporally incorporate peptides and proteins in PEG hydrogels via tetrazine-norbornene addition,[30] CuAAC,[36] or SPAAC.[29,37] Hawker et al. also utilized thiol−ene reactions to immobilize bioactive and diagnostic molecules to hydrogel microarray surfaces.[40] Dynamic 3D patterning of biological cues were developed via CuAAC where Cu(I) was produced by photo-initiated Cu(II) reduction.[34] Shoichet and co-workers further exploited thiol-maleimide Michael-addition for spatial patterning of agarose hydrogels.[41,42]

Recently, the condensation between aldehyde or ketone groups and aminooxy functional groups, which is also known as an oxime ligation, has grown in popularity as an emerging "click" reaction (Figure 2c). It occurs readily in aqueous solutions without major side reactions[43,44] and is used widely for the conjugation and labeling of biological molecules, cell surface modification, scaffolds preparation, and injectable hydrogels.[45−48] Though an oxime bond is more stable than a hydrazone,[43] it has been shown to be reversible in some biologically relevant environments.[49] Oxime ligation is particularly interesting due to its pH-sensitive reaction kinetics, dependence on catalyst concentration, and varying degrees of reversibility.[44,50] For fast reaction speeds, it is necessary to maintain a slightly acidic reaction environment where the

Received: August 1, 2013
Revised: September 16, 2013
Published: September 19, 2013

Scheme 1. (a) Synthesis Route of Bialdehyde-Functionalized PEG Precursor (PEG-bCHO, n = 104); (b) Synthesis Route of 4-Arm Aminooxy Cross-Linker; (c) Chemical Structure of Azide-Aminooxy Extender (Azide-ONH_2); (d) Chemical Structure of Alkene-Aminooxy Extender (Alkene-ONH_2); (e) Model Reaction of Oxime Ligation between PEG-bCHO and *o*-(Pent-4-en-1-yl)hydroxylamine (Intermediate 2)

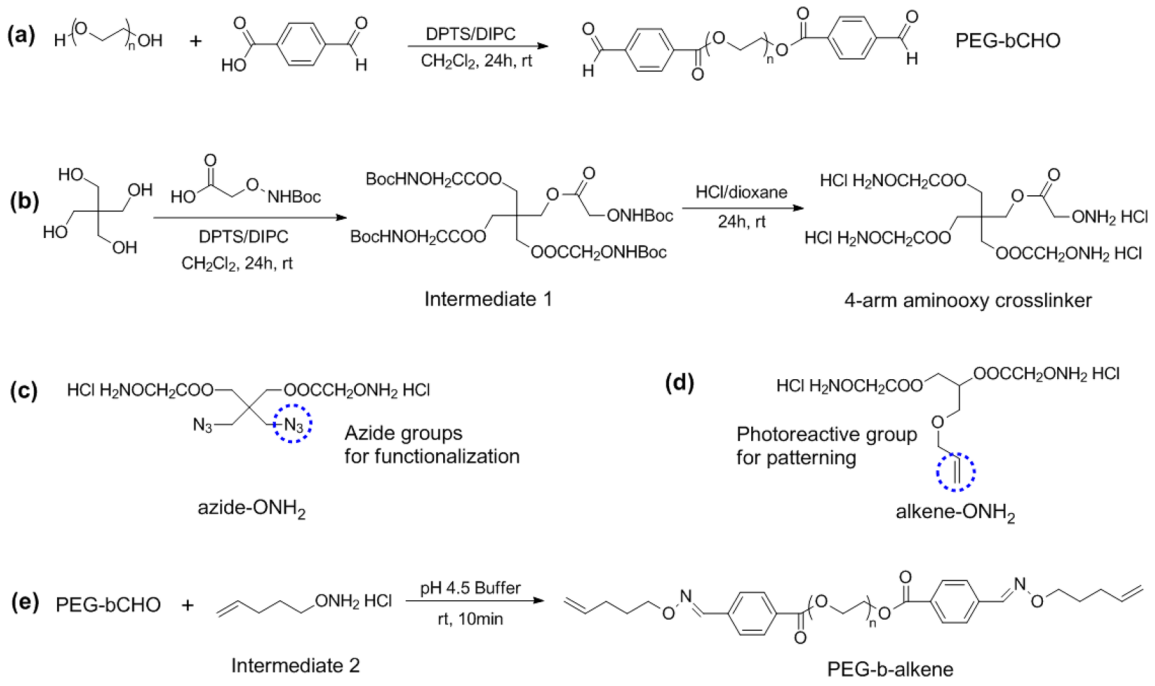

proton serves as a catalyst. In neutral or slightly basic conditions, nucleophilic catalysts such as aniline[44,51] are necessary to obtain the desired reaction rates and extent of conversion. Currently, significant efforts have been focused on the development of nontoxic catalysts, like 4-aminophenylalanine.[52] These unique features inspire us to create hydrogels with tunable properties such as mechanical strength and gelation time by modulating the reaction conditions.

Our experimental results show using oxime ligation to fabrication hydrogels with tunable mechanical and gelation properties, as well as chemical functionalities for postgelation biological cues incorporation is an attractive and highly versatile strategy. We have designed and synthesized two precursors: bialdehyde-functionalized PEG (PEG-bCHO; Figure 2a) and a 4-arm aminooxy cross-linker (Figure 2b) molecule. Using identical precursor compositions, we found that the hydrogel properties were influenced greatly by both pH and the presence or absence of an aniline catalyst. The gelation process was completed in minutes at a pH of 4.5 and the resulting storage modulus was 14 kPa, while at a pH of 7.4, the gelation process takes hours to form a much softer gel with a modulus of 0.3 kPa. The aniline catalyst helped to improve the gel mechanical properties and shorten the gelation process. In addition, azide-functionalized oxime hydrogels were also prepared for post-gelation incorporation of RGD peptides via CuAAC and SPAAC. 3D photo patterning of peptides via thiol−ene chemistry was also explored in alkene derived oxime hydrogels.

MATERIALS AND METHODS

Materials. All commercial reagents and solvents were purchased from Aldrich or Fisher Scientific and used without further purification unless noted otherwise. All reactions were performed under a blanket of nitrogen unless noted otherwise.

Instrumentation. NMR spectra were obtained by Varian NMRS 300 MHz spectrometer. All chemical shifts are reported in ppm (δ) and referenced to the chemical shifts of residual solvent resonances (^{1}H NMR $CDCl_3$ 7.27 ppm, D_2O 4.80 ppm, DMSO-d_6 2.50 ppm); ^{13}C $CDCl_3$ 77.00 ppm, DMSO-d_6 39.50 ppm). The following abbreviations were used to explain the multiplicities: s = singlet, d = doublet, t = triplet, br = broad singlet, and m = multiplet. FT-IR spectra were recorded on a SHIMADZU MIRacle 10 ATR-FTIR, and Raman spectra were recorded on a LabRAM HR 800 spectrophotometer. Fluorescence microscopy images were recorded on OLYMPUS IX 81 Microscope and are unaltered. Size exclusion chromatographic analyses (SEC) were performed using a Waters 150-C Plus instrument equipped with three HR-Styragel columns [100 Å, mixed bed (50/500/103/104 Å), mixed bed (103, 104, 106 Å)], and a differential refractometer (Waters 410) detector. THF was used as eluent with a flow rate of 1.0 mL/min at 30 °C. The molecular mass and mass distribution were calculated from polystyrene standards. Electrospray ionization (ESI) was performed using a HCT Ultra II quadrupole ion trap mass spectrometer (Bruker Daltonics, Billerica, MA) equipped with an electrospray ionization source. MALDI-TOF mass spectra were carried out on a Bruker Ultraflex-III TOF/TOF mass spectrometer (Bruker Daltonics, Inc., Billerica, MA) equipped with a Nd:YAG laser (355 nm); all spectra were measured in positive reflection mode. *trans*-2-[3-(4-*tert*-Butylphenyl)-2-methyl-2-propenylidene]-malononitrile (DCTB, Aldrich, >98%) and sodium trifluoroacetate served as matrix and cationizing salt, respectively (see SI for details).

Synthesis of Bialdehyde-Functionalized PEG Precursor (PEG-bCHO). The synthesis route is described as shown in Scheme 1a. Both PEG (4.6k) and 4-formylbenzoic acid were vacuum-dried overnight prior to use. In a 250 mL round flask, PEG (4600 g/mol, 9.2 g, 2 mmol), 4-(*N*,*N*-dimethylamino)pyridinium-4-toluenesulfonate (DPTS, 0.5 g, 1.5 mmol), and 4-formylbenzoic acid (1.2 g, 8 mmol) were dissolved in 50 mL of anhydrous DMF. The reaction mixture was placed in an ice bath for 10 min, followed by the addition of 1,3-diisopropyl carbodiimide (DIPC, 1.5 mL, 10 mmol) via syringe. The white precipitation was observed in minutes. The reaction was allowed to warm up to room temperature and stir for 24 h. After centrifugation to remove solids, the top layer solution was diluted with 1 L of methanol. The resulting solution was kept at −20 °C overnight. The

dx.doi.org/10.1021/bm401133r | *Biomacromolecules* 2013, 14, 3749−3758

resulting white solid was isolated by centrifugation and washed with cold methanol three times followed by ethyl ether twice. After vacuum drying, a white solid product (8.2 g, yield 82%) was stored at −20 °C for future use. ^{1}H NMR (300 MHz, $CDCl_3$): δ 10.09 (s, 1H, -PhC***H***O), 8.21 (m, 2H, aromatic H), 7.95 (m, 2H, aromatic H), 4.50 (t, 2H, -COOC***H***$_2$CH$_2$O-), 3.84 (t, 2H, -COOCH$_2$C***H***$_2$O-), 3.63 (s, ∼220 H, -C***H***$_2$C***H***$_2$O-, PEG main chain). FT-IR (cm^{-1}): 2881, 1719, 1701, 1466, 1359, 1341, 1279, 1240, 1202, 1145, 1095, 1059, 961, 841, 760, 681.

Synthesis of 4-Arm Aminooxy Cross-Linker. The synthesis route is described as shown in Scheme 1b. Intermediate **1** was first prepared via conventional esterification. Briefly, in a 100 mL round-bottom flask, pentaerythritol (1 g, 7.5 mmol), DPTS (0.25 g, 0.75 mmol), and (Boc-aminooxy)acetic acid (5.8 g, 30 mmol) were dissolved in 30 mL of anhydrous DMF. The reaction mixture was placed in an ice bath for 10 min, followed by the addition of DIPC (5.5 mL, 36 mmol) via syringe. White precipitation was observed within minutes. The reaction formulation was allowed to warm to room temperature and was stirred for 24 h. After removal of the solid by filtration, the collected solution was concentrated for chromatography purification on silica gel (ethyl acetate/hexane = 3:1 (v/v)). The resulting product was a white solid (7.9 g, yield 65%). ^{1}H NMR (300 MHz, $CDCl_3$): δ 7.93 (s, 4H, -N***H***CO-), 4.47 (s, 8H, -NHOC***H***$_2$CO-), 4.26 (s, 8H, -COOC***H***$_2$C-), 1.49 (s, 36H, (C***H***$_3$)$_3$CO). ^{13}C NMR (300 MHz, $CDCl_3$): δ 169.06, 159.27, 82.41, 72.38, 61.91, 42.76, 28.15.

The 4-arm aminooxy cross-linker was achieved through the deprotection of tert-butyloxycarbonyl (BOC) group from intermediate **1**. Briefly, in a 100 mL round-bottom flask, intermediate **1** (2.00 g, 2.4 mmol) was dissolved in HCl/dioxane solution (20 mL, 4 M). The solution was allowed to stir at room temperature for 24 h. The white precipitate was isolated by filtration and washed with dioxane three times followed by ethyl ether twice. After drying in vacuum, product came out as a white solid (1.35 g, quantitative). ^{1}H NMR (300 MHz, $CDCl_3$): δ 4.85 (s, 2H, $^+$NH$_3$OC***H***$_2$CO-), 4.45 (s, 2H, -COOC***H***$_2$C-)). FT-IR (cm^{-1}): 3710−2159 broad, 1743, 1679, 1513, 1409, 1368, 1205, 1115, 1060, 1015, 887, 873, 717.

Synthesis of Azide-aminooxy Extender (Azide-ONH$_2$). The chemical structure of azide-ONH$_2$ is shown in Scheme 1c. It was synthesized in a similar process as 4-arm aminooxy cross-linker. Detailed synthesis procedure was discussed in the Supporting Information. ^{1}H NMR (300 MHz, D_2O): δ 4.67−4.73 (m, 4H, $^+$NH$_3$OC***H***$_2$COO-), 4.15−4.25 (m, 4H, -CH$_2$COOC***H***$_2$C-), 3.42−3.52 (m, 4H, -CC***H***$_2$N$_3$).

Synthesis of Alkene-Aminooxy Extender (Alkene-ONH$_2$). The chemical structure of alkene-ONH$_2$ is shown in Scheme 1d. It was synthesized in a similar process as 4-arm aminooxy cross-linker. Detailed synthesis procedure was discussed in the Supporting Information. ^{1}H NMR (300 MHz, D_2O): 5.75−6.05 (m, 1H, -C***H***═CH$_2$), 5.10−5.50 (m, 3H, -COOCH$_2$C***H***OOC-, -CH═C***H***$_2$), 4.55−4.80 (m, 4H, $^+$NH$_3$OC***H***$_2$COO-), 4.30−4.50 (m, 2H, -COOC***H***$_2$CHOOC-), 3.95−4.15 (m, 2H, -OC***H***$_2$CH═CH$_2$), 3.78 (d, 2H, -CHC***H***$_2$OCH$_2$CH═CH$_2$).

Model Reaction of Oxime Ligation (PEG-*b*-Alkene). The oxime ligation reaction is described in Scheme 1e. In a 4 mL glass vial, PEG-bCHO (100 mg, 0.02 mmol) and *o*-(pent-4-en-1-yl) hydroxylamine (intermediate **2**, Supporting Information; 8.4 mg, 0.06 mmol) was dissolved in acetic buffer (pH 4.5) and stirred at room temperature for 10 min. The reaction mixture was subjected for MALDI-TOF characterization without purification. Pure sample was obtained by dialyzation in deionized water (molecular weight (MW) cut-off 3000 g/mol, cellulose membrane, Pierce), followed by lyophilization. ^{1}H NMR (300 MHz, $CDCl_3$): δ 8.05−8.10 (m, 2H, aromatic H), 7.58−7.68 (m, 2H aromatic H), 5.75−5.95 (m, 1H, CH$_2$═C***H***CH$_2$-), 4.93−5.13 (m, 2H, C***H***$_2$═CHCH$_2$-), 4.40−4.55 (t, 2H, -COOC***H***$_2$CH$_2$O-), 4.15−4.25 (t, 2H, -CH$_2$C***H***$_2$ON═C-), 3.80−3.90 (m, 2H, -COOCH$_2$C***H***$_2$O-), 3.55−3.75 (s, ∼220H, -C***H***$_2$C***H***$_2$O-, PEG main chain), 2.10−2.25 (m, 2H, CH$_2$═CHC***H***$_2$CH$_2$CH$_2$O-), 1.75−1.90 (m, 2H, CH$_2$═CHCH$_2$C***H***$_2$CH$_2$O-).

Synthesis of Functionalized Peptides. Two kinds of peptides bearing "clickable" groups were synthesized via standard solid phase FMOC methodology on a CEM Discovery automated peptide synthesis machine. Peptides were cleaved from resin using standard conditions (45 min, 95% trifluoroacetic acid (TFA), 2.5% triisopropylsilane (TIPS), 2.5% water (by volume)), and precipitated in cold diethyl ether. The crude solid product was isolated by centrifuge, washed twice with diethyl ether, and dialyzed in deionized water (molecular weight (MW) cut off 500 g/mol, cellulose membrane, Pierce), followed by lyophilization. As to alkyne-RGD-biotin (sequence Alkyne-GRGDSK(Biotin)-COOH), 5-hexynoic acid was coupled to N-terminus using standard amino acid coupling condition before cleavage. For fluorescein-5(6)-isothiocyanate (FITC)-RGD-thiol (sequence FTIC-GRGDSCS), FITC (Sigma) was coupled to N-terminus in DMF overnight before cleavage.[53,54] Alkyne-RGD-Biotin: ESI calcd 939.1, found 939.5. FTIC-RGD-thiol: ESI calcd 1070.1, found 1070.5. Excitation 492 nm, emission 512 nm (PBS buffer, pH 7.4).

Hydrogel Fabrication and Characterization. Citrate-phosphate buffer (10 mM) was used with different pH (2.5, 4.5, 6.0, 6.6, 6.8, 7.0, 7.2, 7.4, and 7.6) for hydrogel formation. Hydrochloric acid−potassium chloride buffer (pH 1.5) was used as the highest acid concentration condition. Concentration of the aniline catalyst was controlled as (0.1 wt %) when used. Hydrogels were prepared with the stoichiometric balanced formulations (1:1 total aminooxy/aldehyde), and total precursor concentration was 10 wt %. The two precursors were predissolved separately in the respective buffer solutions to control the pH. Mixing of the two solutions resulted in the formation of oxime hydrogels. For oscillatory shear measurement, mixture of PEG-bCHO solution and 4-arm aminooxy cross-linker solution was placed in a silicon mold for 12 h to make sure the gelation reactions are complete. Hydrogels were then soaked in phosphate buffered saline (PBS, 10 mM, pH 7.0) overnight to reach the swollen equilibrium. The equilibrium modulus measurements were recorded using a ARES G2 Rheometer (TA Instrument) using 8 mm parallel plate geometry at room temperature, and the gel thickness was around 1 mm. Hydrogels were immersed in PBS during the whole testing process. Frequency ramped from 100 to 0.1 rad s^{-1} with 10% strain. To evaluate the gel formation kinetics, storage modulus (G'), and loss modulus (G'') were observed at the constant frequency 10 rad s^{-1} as a function of time with a strain of 10%. The top of gel formulation was covered with silicon oil to avoid dehydration.

Azide-Derived Hydrogel Fabrication and Further Functionalization. The citrate-phosphate buffer (10 mM, pH 4.5) was used as the gelation medium. The ratio between the total aminooxy and aldehyde stoichiometry was controlled precisely at 1:1. The concentration of PEGs was 10 wt %. First the PEGs and biaminooxy extender (0.1 equiv to aldehyde) were mixed in buffer solution and stirred for 10 min, followed by the addition of the 4-arm aminooxy cross-linker (0.9 equiv to aldehyde) solution. After 12 h of gelation time, the hydrogels were immersed in PBS (pH 7.0) overnight to reach the swollen equilibrium for further peptide functionalization.

Azide hydrogels were incubated overnight in alkyne-RGD-biotin solution (1 mg/mL) in PBS, together with copper sulfate (0.1 mg/mL) and sodium ascorbate (1 mg/mL). Hydrogels were then placed in fresh media for 2 d to remove copper salt and any unbonded peptides. For FT-IR testing, the solvent exchange was further carried out in deionized water for 1 d before lyophilization. The dried gel sponge was then characterized by FT-IR.

For the protein binding assay, after the copper salt removal, peptide-functionalized hydrogels were incubated in tetramethylrhodamine-5(6)-isothiocyanate (TRITC)-labeled streptavidin PBS solution (10 ug/mL) for 2 h, followed by incubation in fresh media overnight to remove unbound protein. The resulting hydrogels were imaged by fluorescence microscopy. A control experiment was conducted with plain azide gel without peptide conjugation.

Alkene-Derived Hydrogels Fabrication and 3D Biochemical Patterning. Alkene hydrogels were fabricated similarly to azide hydrogels with the exception of using an alkene aminooxy extender to replace the azide one. The thickness of the hydrogel was 1 mm or less. Alkene hydrogels were incubated in PBS containing Irgacure 2959 (0.1 mg/mL) and the patterning agent FTIC-RGD-thiol (0.01 mg/mL) for

30 min. Using conventional photolithographic techniques, gels were exposed to ultraviolet light (365 nm wavelength) through a 300 mesh TEM grid mask for 2 min. After the patterning was complete, hydrogels were washed overnight with fresh media to remove any unbound peptides. The final patterned hydrogels were imaged by fluorescence microscopy.

RESULTS AND DISCUSSION

Hydrogel Precursor Synthesis. Bis-aldehyde-functionalized PEG (PEG-bCHO) was synthesized via carbodiimide coupling with 4-formylbenzoic acid, in the presence of DPTS and DIPC. The aldehyde group of 4-formylbenzoic acid is highly reactive due to electron deficiency. DPTS/DIPC was employed as catalyst system to obtain high reaction efficiency and yields under mild conditions.[55] The complete conversion of hydroxyl to aldehyde was verified by matrix-assisted desorption ionization time-of-flight mass spectrometry (MALDI-TOF-MS, Figure 1a), which shows a single distribution. The monoisotopic mass of each peak matches well with that expected for PEG-bCHO (e.g., for [103mer +Na]$^+$, found 4839.7 Da vs calcd 4839.6 Da). The difference between neighboring peaks is equal to the mass of a -CH_2CH_2O- repeating unit (44.0 Da). Analysis by size-exclusion chromatography (SEC) with polystyrene standard indicated a number average molecular weight (M_n) of 5200 Da (polydispersity index (PDI) = 1.08; Supporting Information, Figure S1, Table S1). It is higher than the M_n of PEG raw materials, which was measured to be 4860 Da.

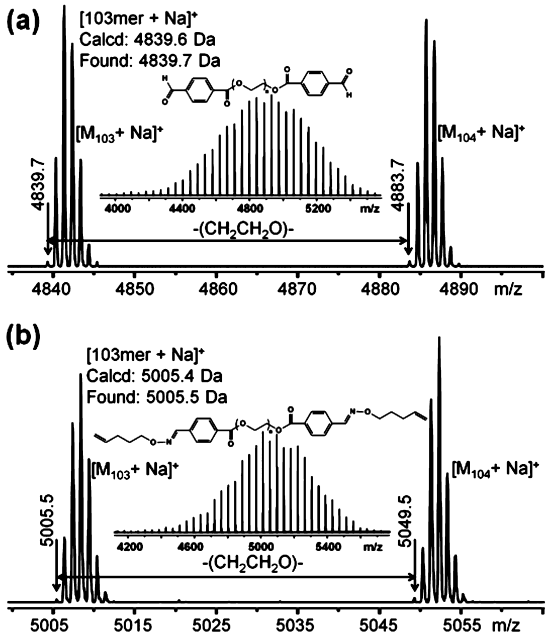

Figure 1. MALDI-TOF mass spectra of (a) bialdehyde-functionalized PEG (PEG-bCHO); (b) Model reaction product between PEG-bCHO and *o*-(pent-4-en-1-yl)hydroxylamine (intermediate **2**) showing a monomodal distributions and complete reaction conversion.

Prior to hydrogel fabrication, a model reaction was conducted to verify the reaction efficiency and reaction rate of oxime ligation. Intermediate **2** (Supporting Information) was used as a model substrate and coupled to PEG-bCHO in pH 4.5 buffer solution. The raw formulation was submitted to MALDI-TOF-MS without purification after mixing the reagents for 10 min. The single monomodal distribution of the mass spectra (Figure 1b) demonstrates the complete conversion of aldehyde to oxime. The monoisotopic mass peak at 5005.5 Da in Figure 1b corresponds to the peak at 4839.7 Da in Figure 1a after end-capping with *o*-(pent-4-en-1-yl)hydroxylamine. In SEC analysis, the M_n of the PEG-*b*-alkene is 5390 Da (PDI = 1.12; Supporting Information, Figure S1, Table S1). The exhibited fast reaction rate and high reaction efficiency of the oxime ligation outlined the promising strategy to fabricate the hydrogels.

Hydrogel Fabrication and Chemical Characterization. Hydrogels were formed using a 10% (mass) precursor solution containing a 1:1 ratio of aldehyde to aminooxy functionalities (Figure 2d). FT-IR was used to examine the chemical structure of resulted hydrogels. In Figure 2g, both the aldehyde C═O stretch at 1701 cm^{-1} and the C−C stretch at 1202 cm^{-1} (black line) of PEG-bCHO are much weaker in the spectra of cross-linked hydrogels (red line), indicating that the high conversion of the aldehyde groups was achieved in the network formation process. A new stretch at 1762 cm^{-1} within the hydrogels is assigned to the ester C═O stretch of the 4-arm aminooxy cross-linker. Raman spectroscopy was also used to further verify this cross-linking process (Figure 2h). The characteristic stretch of the oxime C═N bond is found as a sharp peak at 1612 cm^{-1} (red line). Meanwhile, the small peak at 1612 cm^{-1} (black line) is assigned to the phenyl stretch of PEG-bCHO, which is shifted to 1565 cm^{-1} (red line) after the oxime ligation due to the conjugation of π electrons.[56]

pH Control Over Hydrogel Mechanical Properties and Gelation Kinetics. It is very important to control the intrinsic mechanical properties of the hydrogels, which would influence the interaction between the scaffolds and surrounding biological environment, including cell behavior, gene expression, and tissue regeneration.[57−60] Recently we have shown that mechanical properties of polyethylene glycol dimethacrylate (PEGDM) hydrogels have a significant impact in modulating human osteoarthritic chondrocyte behaviors and tissue formation.[9] In addition, recent reports by Ifkovitsa and co-workers found that injectable hyaluronic acid hydrogels with high mechanical strength can improve the postmyocardial infarction remodeling process.[61]

To quantitate the influence of pH on hydrogel formation, a series of buffer solutions with different pH values, from 1.5 to 7.6, were used as the gel formation media. The gel precursor composition was kept identical (10%, mass), as well as the 1:1 ratio of aldehyde to aminooxy functional groups. Figure 3a shows the modulus-frequency curves of two hydrogels formed in buffer at two different pH values. At a pH of 4.5, the resulting gel has a storage modulus 14.1 ± 1.2 kPa. It is nearly 50 times stronger than the gel formed at pH of 7.4, which resulted in a storage modulus of only 0.3 ± 0.1 kPa. Figure 2e,f demonstrates the strength difference by appearance. The plot in Figure 3b shows the pH control over the resulting storage modulus. In the first region from pH 1.5 to 4.5, the storage modulus increases with increasing pH. In the pH range between 4.5 and 7.4, the storage modulus decreases with an increase in pH, especially in slightly basic environments. The storage modulus of gels at pH of 7.0 is 6.2 ± 0.9 kPa, while at pH of 7.4, it drops to 0.3 ± 0.1 kPa. There is no coherent hydrogel formation at pH 7.6, which results in a very viscous fluid.

The mechanical strength of the hydrogels is directly related to the cross-link density, which is determined by functional group conversion. The theoretical gel-point conversion for the

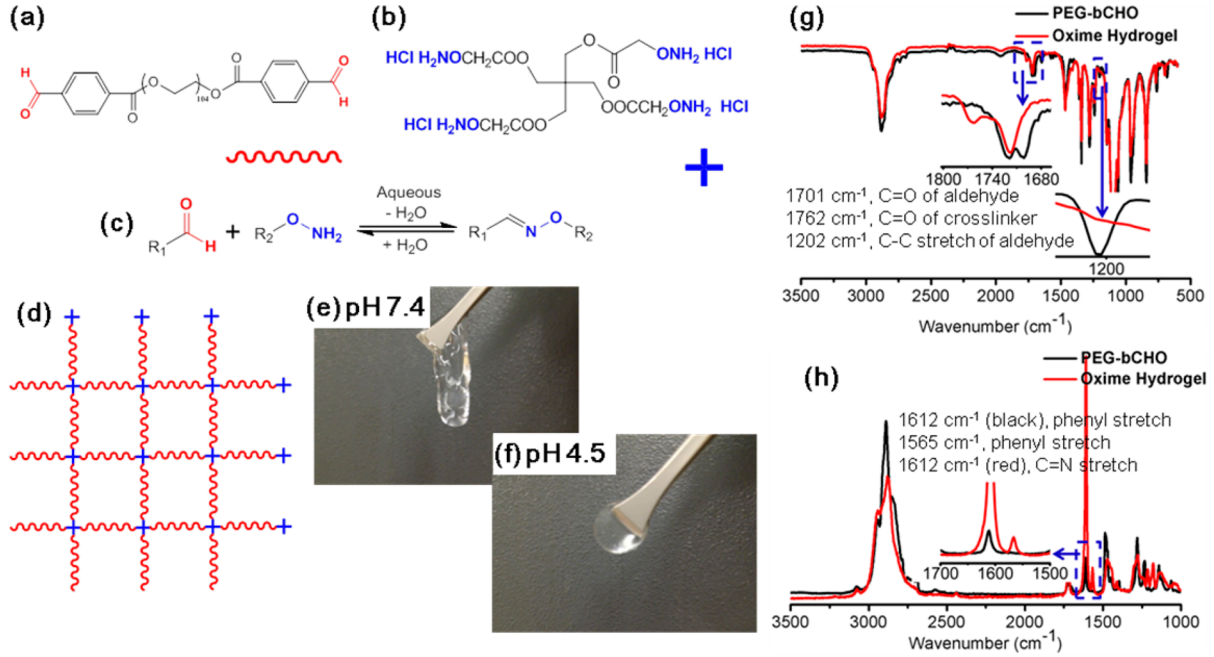

Figure 2. (a) Chemical structure of bialdehyde-functionalized PEG (PEG-bCHO). (b) Chemical structure of 4-arm aminooxy cross-linker. (c) General reaction scheme for theoxime ligations. The reaction is pH and nucleophile catalyst dependent. (d) Schematic of the hydrogel network formation via oxime bond ligation using a 4-arm aminooxy cross-linker. (e) Photos of hydrogels formed at pH 7.4 and hydrogels formed at pH 4.5 (f) show clearly the mechanical differences in the hydrogels with the fast cross-linking kinetics. Gels obtained at pH 4.5 are stronger than those at pH 7.4 at similar time intervals. (g) FT-IR spectra of PEG-bCHO (black) and hydrogels (red) clearly show the extent of oxime formation in the hydrogels. (h) Raman spectra of phenyl and C═N transitions for PEG-bCHO (black) and hydrogels (red) compliment the FT-IR data showing the extent of reaction during the gel formation.

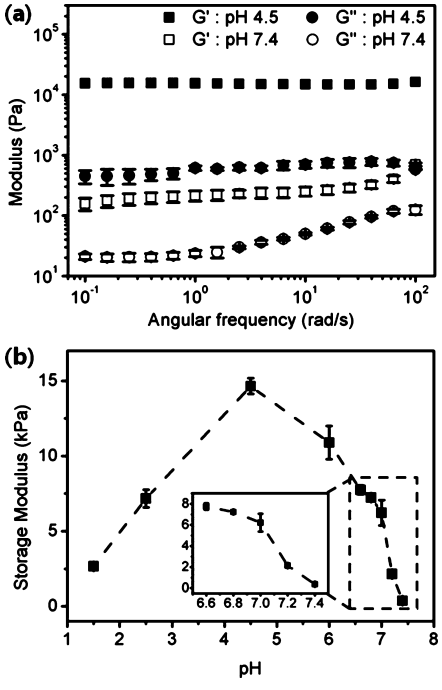

Figure 3. Extent of cross-linking and mechanical properties are highly dependent on pH. (a) Modulus vs frequency behavior of hydrogels formed at pH 4.5 and 7.4 show that the gels formed at low pH are much stronger at comparable time intervals; (b) The storage modulus (G')−pH plot (frequency 10 rad/s, strain 10%) show that the mechanical properties can be tuned via pH. The data are displayed as the mean and the error bars represent the standard deviation of three independent measurements for each condition.

step-growth polymerization can be calculated by the Flory−Stockmayer equation[62,63]

$$\rho = \frac{1}{\sqrt{r(1 - f_{\text{aldehyde}})(1 - f_{\text{aminooxy}})}} \quad (1)$$

where ρ is the gel-point conversion, r is the stoichiometric ratio, and f_{aldehyde} and f_{aminooxy} are the degree of functionality for PEG-bCHO and 4-arm linker, respectively. In the current system, we have $r = 1$, $f_{\text{aldehyde}} = 2$, and $f_{\text{aminooxy}} = 4$. The critical conversion is approximately 0.58 to achieve gelation. As to oxime ligation, the reaction conversion and equilibrium is largely influenced by pH.[44,50] When pH decreases from 4.5 to 1.5, the reverse reactions are favored due to the protonation of imines (pKb ∼ 10), which is the rate-limiting step for oxime hydrolysis. The equilibrium of the oxime ligation shifts to the left and the functional group conversion and cross-link density are reduced. As a result, the obtained hydrogels are softer and have a smaller storage modulus. Meanwhile, at pH values of 1.5 and 2.5, the gel was formed immediately after mixing the two precursors (see gelation kinetic data, Figure 4b). The fast gelation largely restricts the mobility of both aldehyde and aminooxy, and further cross-link density is reduced. On the other hand, fast gelation results in microscopic inhomogeneity and then leads to weaker hydrogels.[64] In the pH range from 4.5 to 7.6, the reaction conversion is reduced due to the increase of pH, and the critical conversion is never reached at pH 7.6. The optimal environment for oxime ligation is mildly acidic. Under these conditions, the attenuated basicity of the aminooxy groups leaves it unprotonated for further attack on the aldehyde, and the imine is also unprotonated due to the α-effect,[65] which suspends the hydrolysis process.

dx.doi.org/10.1021/bm401133r | Biomacromolecules 2013, 14, 3749−3758

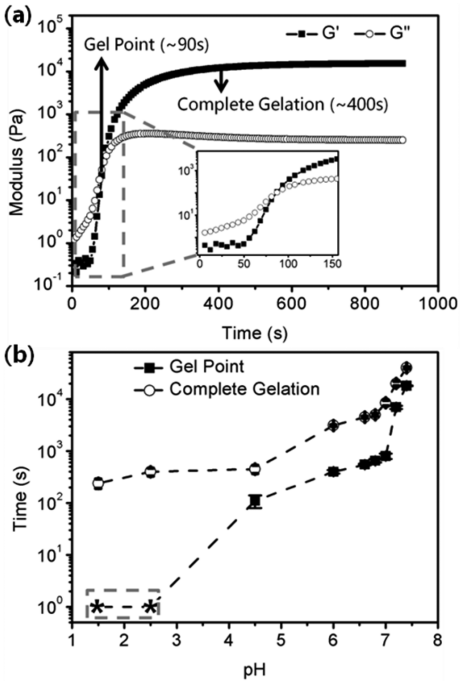

Figure 4. Gelation kinetics are highly dependent on pH. (a) Modulus-time behavior of hydrogels formed at pH 4.5; (b) Plot of pH vs time captures the gel point and the times to reach complete gelation. At low pH the gelation time is too fast to capture. The asterisks (*) in (b) represent time intervals that are too short to detect. The data represent the mean and the error bars represent the standard deviation of three independent samples for each condition.

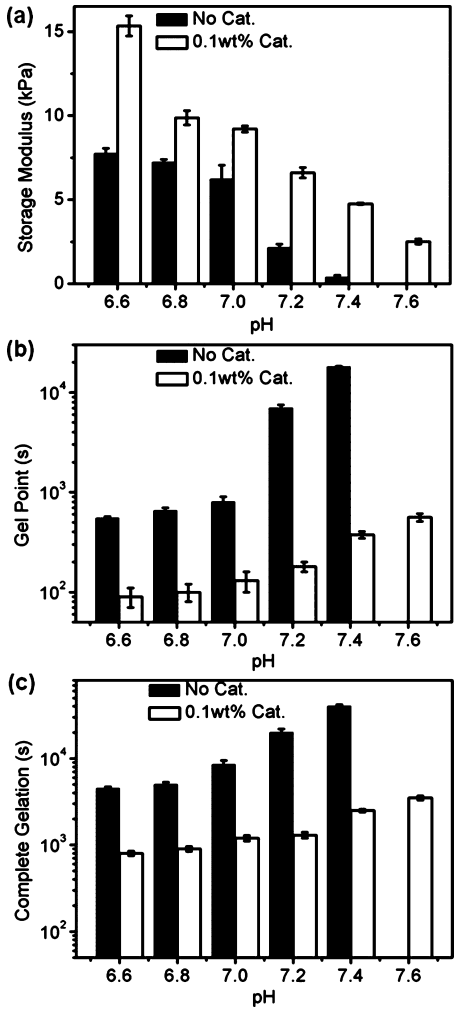

Figure 5. Influence of aniline catalyst (0.1 wt %) on hydrogels storage modulus (a), time to reach the gel point (b), and the complete gelation time (c) as a function of pH. The data represent the mean and the error bars represent the standard deviation of three independent samples for each condition.

In the time-dependent gelation experiment (Figure 4a), the crossover of storage modulus (G') and loss modulus (G'') represents the gel point, which means the transformation from a viscous liquid to a viscoelastic solid. The storage modulus plateau is treated as the complete gelation. In the entire pH range we tested, from strongly acidic to slightly basic, a decrease in acid concentration lead to the faster gel point and complete gelation time (Figure 4b). At pH 1.5 and 2.5, the gel point is not detected due to the fast gelation behavior; only the complete gelation time is obtained (240 s at pH 1.5 and 400 s at pH 2.5). At pH 7.4, the gel point is achieved after 5 h, and 10 h is required for complete gelation. This process is kinetically controlled. The oxime bond formation is catalyzed by acid, which activates aldehyde by protonation and accelerates the dehydration step. When pH decreases, the reaction rate is increased, and then the critical conversion 0.58 and final conversion is achieved faster. It indicates that less time for gelation point and complete gelation is required.

Influence of Aniline Catalyst on Hydrogel Mechanical Properties and Gelation Kinetics. Additional studies quantified the influence of the nucleophilic catalyst, aniline, on hydrogel mechanical properties, and the gelation behavior with a pH ranging from 6.6 to 7.6. Aniline is a widely used catalyst for oxime gelation and has been shown to improve the reaction rate and efficiency.[44,66] As shown in Figure 5a, aniline greatly influences the mechanical strength of hydrogels. The catalyst leads to a large increase in the storage modulus, especially at neutral and slightly basic conditions. At pH 7.4, the storage modulus of hydrogels with aniline is 4.7 ± 0.3 kPa, while the storage modulus without aniline is only 0.3 ± 0.1 kPa. Particularly at pH 7.6, there was no gel formation in the absence of catalyst. Following the addition of catalyst, gels with the storage modulus of 2.4 ± 0.2 kPa were obtained. The gelation kinetics are also catalyst-dependent. The time scale of both the gel point (Figure 5b) and time to complete gelation (Figure 5c) is reduced from hours to minutes with the addition of aniline. Adding catalyst results in stronger hydrogels by increasing the functional group conversion and cross-link density and enables the critical conversion to be reached at pH 7.6. At the same time, aniline also accelerates oxime ligation, and reduces the time necessary to achieve critical conversion.[44,51]

Oxime Hydrogels with Chemical Functionalities and Its Further Derivation with Peptides. Azide- and alkene-functionalized hydrogels were prepared for further conjugation of biological molecules via a cascade approach as shown in Figure 6a. The 2-arm aminooxy precursor with azide (azide-ONH_2, Scheme 1c) or alkene (Scheme 1d) handles was used as the chain extender. It reacted with PEG-bCHO, resulting in a new precursor formulation in situ. Aldehyde groups are present on the chain end, while the other two arms contain azide or alkene groups. The content of the PEG with "clickable" groups in aldehyde mixtures was controlled via feed ratio between the

dx.doi.org/10.1021/bm401133r | Biomacromolecules 2013, 14, 3749−3758

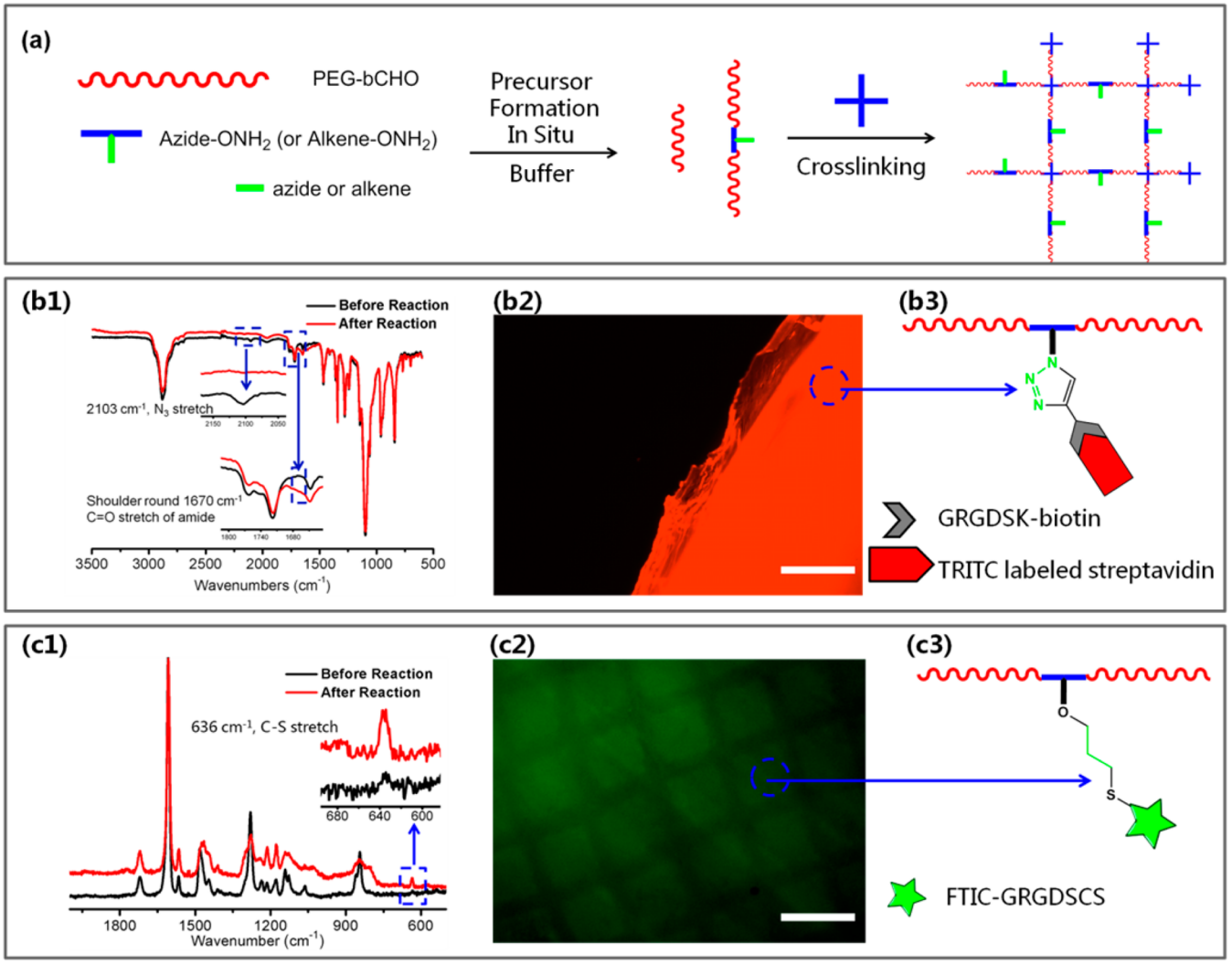

Figure 6. (a) Fabrication procedure of oxime hydrogels with "clickable" groups is a two-step process. PEG-bCHO was initially mixed together with azide-ONH_2 (or alkene-ONH_2) for minutes, followed by the addition of 4-arm aminooxy cross-linker. (b1) FT-IR spectra of azide-functionalized hydrogels before (black) and after (red) "click" conjugation with alkyne-RGD-biotin peptides. (b2) Fluorescence microscopy image of azide hydrogels after bonding with TRITC-labeled streptavidin. Red areas are from labeled hydrogels and black areas are the glass side background. (b3) Schematic of the "click" cycloaddition reaction and the binding sites for peptide or protein conjugation. (c1) Raman spectra of alkene hydrogels before (black) and after (red) the thiol−ene addition of 2-mercaptoethanol. (c2) Fluorescence microscopy image of alkene-functionalized hydrogels after 3D patterning with FTIC-RGD-thiol. (c3) Schematic of thiol−ene addition sites (scale bar = 100 um).

extender and PEG-bCHO. The 4-arm cross-linker solution was added into aldehyde mixtures to form cross-linked hydrogels.

Azide incorporation into oxime hydrogels was confirmed via FT-IR spectroscopy. The characteristic azide stretch peak is present at 2103 cm^{-1} (Figure 6b1, black line). Azide groups provide a platform to functionalize hydrogels using azide−alkyne Huisgen cycloaddition, which is widely used in biomedical engineering for bioconjugation and tissue labeling applications.[67−70] Alkyne-RGD-biotin was used as a model peptide to verify the availability of azide groups for postgelation reactions. The disappearance of the azide stretch peak after the "click" cyclization reaction indicates the peptide incorporation into hydrogel matrix was successful (Figure 6b1, red line). An additional protein binding experiment was conducted with tetramethylrhodamine-5(6)-isothiocyanate (TRITC) labeled streptavidin.[71,72] The strong red fluorescence of labeled streptavadin protein confirms the existence and bioavailability of biotin in the hydrogels (Figure 6b2). The dark region is the glass slide background. The reaction and binding sites are described in Figure 6b3. The azide-derivatized hydrogels also showed chemical reactivity with 4-dibenzocyclooctynol-derived PEG[39] via SPAAC (data not shown).

Oxime hydrogels bearing alkene groups were also utilized for peptide conjugation via photoinitiated thiol−ene reactions. In the Raman spectra of the alkene-functionalized gels in Figure 6c1 (black line), the stretch of the alkene is not observed due to the overlap with the imine peak between 1600 and 1700 cm^{-1}. Following the photoinitiated addition of 2-mercaptoethanol with Irgacure 2959 as the radical formation initiator, the C−S stretch peak at 630 cm^{-1} is observed (Figure 6c1, red line), which indicates the occurrence of the thiol−ene radical addition. This reaction is further used to create spatial patterns of peptides in oxime hydrogels using a simple photomask. Fluorescein-5-isothiocyanate (FTIC) conjugated RGD with pendant thiol groups (FTIC-RGD-SH) was employed as the model bioactive signal to explore the potential for photochemical patterning. Photocoupling was achieved using a UV light source (365 nm) and the biocompatible initiator Irgacure

dx.doi.org/10.1021/bm401133r | Biomacromolecules 2013, 14, 3749−3758

2959. A square pattern of fluorescent-labeled peptide was generated with a 300 mesh TEM copper grid functioning as a mask (Figure 6c2). The contrast of the exposed square areas and covered lines is obvious, although background fluorescence was observed due to light scattering in the photo pattering process. The tethered sites are described in Figure 6c3.

CONCLUSION

In conclusion, we have demonstrated the fabrication of covalently cross-linked PEG-based hydrogels via oxime ligation. The cross-linking process is both pH and catalyst dependent. The tunable mechanical properties are related to the condensation equilibrium, reaction rate and the precursors mobility.[73] The results demonstrate that oxime ligation is an efficient method for the fabrication of hydrogels with variable mechanical and gelation kinetics using identical precursors. At 10 wt % concentrations, the storage modulus can be controllably varied from 0.3 to 15 kPa, and the gel formation times can be tuned from seconds to hours. Oxime hydrogels with controlled amounts of residual azide and alkene groups were also obtained. The hydrogels were successfully used for pattern formation and peptide incorporation via robust and highly efficient reaction conditions. These materials are the initial demonstration for translationally relevant hydrogel materials that possess tunable mechanical regimes attractive to soft tissue engineering and possess atom neutral chemistries attractive for post-gelation patterning in the presence or absence of cells.

ASSOCIATED CONTENT

Supporting Information

All synthesis and characterization details of all molecules. This material is available free of charge via the Internet at http://pubs.acs.org.

AUTHOR INFORMATION

Corresponding Author

*E-mail: becker@uakron.edu.

Notes

The authors declare no competing financial interest.

ACKNOWLEDGMENTS

The authors gratefully acknowledge financial support from the Akron Functional Materials Center, RESBIO: Integrated Technologies for Polymeric Biomaterials (NIH-NIBIB P41 EB001046), and the National Science Foundation (CHE-1012636 to C.W.). The authors also acknowledge partial support for A.D. from the NSF (DMR- 1105370).

REFERENCES

(1) Qiu, Y.; Park, K. Environment-Sensitive Hydrogels for Drug Delivery. *Adv. Drug Delivery Rev.* **2001**, *53* (3), 321−339.
(2) Slaughter, B. V.; Khurshid, S. S.; Fisher, O. Z.; Khademhosseini, A.; Peppas, N. A. Hydrogels in Regenerative Medicine. *Adv. Mater.* **2009**, *21* (32−33), 3307−3329.
(3) Lee, K. Y.; Mooney, D. J. Hydrogels for Tissue Engineering. *Chem. Rev.* **2001**, *101* (7), 1869−1880.
(4) Dong, L.; Agarwal, A. K.; Beebe, D. J.; Jiang, H. Adaptive Liquid Microlenses Activated by Stimuli-Responsive Hydrogels. *Nature* **2006**, *442* (7102), 551−554.
(5) Hoare, T. R.; Kohane, D. S. Hydrogels in Drug Delivery: Progress and Challenges. *Polymer* **2008**, *49* (8), 1993−2007.
(6) Nemir, S.; West, J. Synthetic Materials in the Study of Cell Response to Substrate Rigidity. *Ann. Biomed. Eng.* **2010**, *38* (1), 2−20.
(7) Nemir, S.; Hayenga, H. N.; West, J. L. PEGDA Hydrogels with Patterned Elasticity: Novel Tools for the Study of Cell Response to Substrate Rigidity. *Biotechnol. Bioeng.* **2010**, *105* (3), 636−644.
(8) Carr, L. R.; Krause, J. E.; Ella-Menye, J.-R.; Jiang, S. Single Nonfouling Hydrogels with Mechanical and Chemical Functionality Gradients. *Biomaterials* **2011**, *32* (33), 8456−8461.
(9) Smith Callahan, L. A.; Ganios, A. M.; Childers, E. P.; Weiner, S. D.; Becker, M. L. Primary Human Chondrocyte Extracellular Matrix Formation and Phenotype Maintenance Using RGD-Derivatized PEGDM Hydrogels Possessing a Continuous Young's Modulus Gradient. *Acta Biomater.* **2013**, *9* (4), 6095−6104.
(10) Cloyd, J.; Malhotra, N.; Weng, L.; Chen, W.; Mauck, R.; Elliott, D. Material Properties in Unconfined Compression of Human Nucleus Pulposus, Injectable Hyaluronic Acid-Based Hydrogels and Tissue Engineering Scaffolds. *Eur. Spine J.* **2007**, *16* (11), 1892−1898.
(11) Seal, B. L.; Otero, T. C.; Panitch, A. Polymeric Biomaterials for Tissue and Organ Regeneration. *Mater. Sci. Eng., R* **2001**, *34* (4−5), 147−230.
(12) Jeon, O.; Bouhadir, K. H.; Mansour, J. M.; Alsberg, E. Photocrosslinked Alginate Hydrogels with Tunable Biodegradation Rates and Mechanical Properties. *Biomaterials* **2009**, *30* (14), 2724−2734.
(13) Forget, A.; Christensen, J.; Lüdeke, S.; Kohler, E.; Tobias, S.; Matloubi, M.; Thomann, R.; Shastri, V. P. Polysaccharide Hydrogels with Tunable Stiffness and Provasculogenic Properties via α-Helix to β-Sheet Switch in Secondary Structure. *Proc. Natl. Acad. Sci. U.S.A.* **2013**, *110* (32), 12887−12892.
(14) Herrick, W. G.; Nguyen, T. V.; Sleiman, M.; McRae, S.; Emrick, T. S.; Peyton, S. R. PEG-Phosphorylcholine Hydrogels As Tunable and Versatile Platforms for Mechanobiology. *Biomacromolecules* **2013**, *14* (7), 2294−2304.
(15) Song, F.; Zhang, L.-M. Enzyme-Catalyzed Formation and Structure Characteristics of A Protein-Based Hydrogel. *J. Phys. Chem. B* **2008**, *112* (44), 13749−13755.
(16) Nguyen, M. K.; Lee, D. S. Oligo(amidoamine)s Hydrogels with Tunable Gel Properties. *Chem. Commun.* **2010**, *46* (20), 3583−3585.
(17) Mano, J. F.; Sousa, R. A.; Boesel, L. F.; Neves, N. M.; Reis, R. L. Bioinert, Biodegradable and Injectable Polymeric Matrix Composites for Hard Tissue Replacement: State of the Art and Recent Developments. *Compos. Sci. Technol.* **2004**, *64* (6), 789−817.
(18) Zhu, J. Bioactive Modification of Poly(ethylene glycol) Hydrogels for Tissue Engineering. *Biomaterials* **2010**, *31* (17), 4639−4656.
(19) Browning, M. B.; Russell, B.; Rivera, J.; Höök, M.; Cosgriff-Hernandez, E. M. Bioactive Hydrogels with Enhanced Initial and Sustained Cell Interactions. *Biomacromolecules* **2013**, *14* (7), 2225−2233.
(20) Sawhney, A. S.; Pathak, C. P.; Hubbell, J. A. Bioerodible Hydrogels Based on Photopolymerized Poly(ethylene glycol)-*co*-poly(α-hydroxy acid) Diacrylate Macromers. *Macromolecules* **1993**, *26* (4), 581−587.
(21) Elisseeff, J.; McIntosh, W.; Anseth, K.; Riley, S.; Ragan, P.; Langer, R. Photoencapsulation of Chondrocytes in Poly(ethylene oxide)-Based Semi-Interpenetrating Networks. *J. Biomed. Mater. Res.* **2000**, *51* (2), 164−171.
(22) Callahan, L. A. S.; Ganios, A. M.; McBurney, D. L.; Dilisio, M. F.; Weiner, S. D.; Horton, W. E.; Becker, M. L. ECM Production of Primary Human and Bovine Chondrocytes in Hybrid PEG Hydrogels Containing Type I Collagen and Hyaluronic Acid. *Biomacromolecules* **2012**, *13* (5), 1625−1631.
(23) Nimmo, C. M.; Shoichet, M. S. Regenerative Biomaterials that "Click": Simple, Aqueous-Based Protocols for Hydrogel Synthesis, Surface Immobilization, and 3D Patterning. *Bioconjugate Chem.* **2011**, *22* (11), 2199−2209.
(24) Azagarsamy, M. A.; Anseth, K. S. Bioorthogonal Click Chemistry: An Indispensable Tool to Create Multifaceted Cell Culture Scaffolds. *ACS Macro Lett.* **2012**, *2* (1), 5−9.

(25) Elbert, D. L.; Pratt, A. B.; Lutolf, M. P.; Halstenberg, S.; Hubbell, J. A. Protein Delivery from Materials Formed by Self-Selective Conjugate Addition Reactions. *J. Controlled Release* **2001**, *76* (1−2), 11−25.
(26) Pritchard, C. D.; O'Shea, T. M.; Siegwart, D. J.; Calo, E.; Anderson, D. G.; Reynolds, F. M.; Thomas, J. A.; Slotkin, J. R.; Woodard, E. J.; Langer, R. An Injectable Thiol-Acrylate Poly(ethylene glycol) Hydrogel for Sustained Release of Methylprednisolone Sodium Succinate. *Biomaterials* **2011**, *32* (2), 587−597.
(27) Lutolf, M. P.; Lauer-Fields, J. L.; Schmoekel, H. G.; Metters, A. T.; Weber, F. E.; Fields, G. B.; Hubbell, J. A. Synthetic Matrix Metalloproteinase-Sensitive Hydrogels for the Conduction of Tissue Regeneration: Engineering Cell-Invasion Characteristics. *Proc. Natl. Acad. Sci. U.S.A.* **2003**, *100* (9), 5413−5418.
(28) Lin, C.-C.; Raza, A.; Shih, H. PEG Hydrogels Formed by Thiol-Ene Photo-Click Chemistry and Their Effect on the Formation and Recovery of Insulin-Secreting Cell Spheroids. *Biomaterials* **2011**, *32* (36), 9685−9695.
(29) Fairbanks, B. D.; Schwartz, M. P.; Halevi, A. E.; Nuttelman, C. R.; Bowman, C. N.; Anseth, K. S. A Versatile Synthetic Extracellular Matrix Mimic via Thiol-Norbornene Photopolymerization. *Adv. Mater.* **2009**, *21* (48), 5005−5010.
(30) Alge, D. L.; Azagarsamy, M. A.; Donohue, D. F.; Anseth, K. S. Synthetically Tractable Click Hydrogels for Three-Dimensional Cell Culture Formed Using Tetrazine−Norbornene Chemistry. *Biomacromolecules* **2013**, *14* (4), 949−953.
(31) Zhou, H.; Woo, J.; Cok, A. M.; Wang, M.; Olsen, B. D.; Johnson, J. A. Counting Primary Loops in Polymer Gels. *Proc. Natl. Acad. Sci. U.S.A.* **2012**, *109* (47), 19119−19124.
(32) Fan, Y.; Deng, C.; Cheng, R.; Meng, F.; Zhong, Z. In Situ Forming Hydrogels via Catalyst-Free and Bioorthogonal "Tetrazole−Alkene" Photo-Click Chemistry. *Biomacromolecules* **2013**, *14* (8), 2814−2821.
(33) Truong, V.; Blakey, I.; Whittaker, A. K. Hydrophilic and Amphiphilic Polyethylene Glycol-Based Hydrogels with Tunable Degradability Prepared by "Click" Chemistry. *Biomacromolecules* **2012**, *13* (12), 4012−4021.
(34) Adzima, B. J.; Tao, Y.; Kloxin, C. J.; DeForest, C. A.; Anseth, K. S.; Bowman, C. N. Spatial and Temporal Control of the Alkyne−Azide Cycloaddition by Photoinitiated Cu(II) Reduction. *Nat. Chem.* **2011**, *3* (3), 256−259.
(35) Hu, X.; Li, D.; Zhou, F.; Gao, C. Biological Hydrogel Synthesized from Hyaluronic Acid, Gelatin, and Chondroitin Sulfate by Click Chemistry. *Acta Biomater.* **2011**, *7* (4), 1618−1626.
(36) Polizzotti, B. D.; Fairbanks, B. D.; Anseth, K. S. Three-Dimensional Biochemical Patterning of Click-Based Composite Hydrogels via Thiolene Photopolymerization. *Biomacromolecules* **2008**, *9* (4), 1084−1087.
(37) DeForest, C. A.; Polizzotti, B. D.; Anseth, K. S. Sequential Click Reactions for Synthesizing and Patterning Three-Dimensional Cell Microenvironments. *Nat. Mater.* **2009**, *8* (8), 659−664.
(38) DeForest, C. A.; Sims, E. A.; Anseth, K. S. Peptide-Functionalized Click Hydrogels with Independently Tunable Mechanics and Chemical Functionality for 3D Cell Culture. *Chem. Mater.* **2010**, *22* (16), 4783−4790.
(39) Zheng, J.; Smith Callahan, L. A.; Hao, J.; Guo, K.; Wesdemiotis, C.; Weiss, R. A.; Becker, M. L. Strain-Promoted Cross-Linking of PEG-Based Hydrogels via Copper-Free Cycloaddition. *ACS Macro Lett.* **2012**, *1* (8), 1071−1073.
(40) Gupta, N.; Lin, B. F.; Campos, L. M.; Dimitriou, M. D.; Hikita, S. T.; Treat, N. D.; Tirrell, M. V.; Clegg, D. O.; Kramer, E. J.; Hawker, C. J. A Versatile Approach to High-Throughput Microarrays Using Thiol−Ene Chemistry. *Nat. Chem.* **2012**, *4* (5), 424−424.
(41) Wosnick, J. H.; Shoichet, M. S. Three-Dimensional Chemical Patterning of Transparent Hydrogels. *Chem. Mater.* **2007**, *20* (1), 55−60.
(42) Wylie, R. G.; Shoichet, M. S. Three-Dimensional Spatial Patterning of Proteins in Hydrogels. *Biomacromolecules* **2011**, *12* (10), 3789−3796.
(43) Kalia, J.; Raines, R. T. Hydrolytic Stability of Hydrazones and Oximes. *Angew. Chem., Int. Ed.* **2008**, *47* (39), 7523−7526.
(44) Dirksen, A.; Hackeng, T. M.; Dawson, P. E. Nucleophilic Catalysis of Oxime Ligation. *Angew. Chem., Int. Ed.* **2006**, *45* (45), 7581−7584.
(45) Zeng, Y.; Ramya, T. N. C.; Dirksen, A.; Dawson, P. E.; Paulson, J. C. High-Efficiency Labeling of Sialylated Glycoproteins on Living Cells. *Nat. Methods* **2009**, *6* (3), 207−209.
(46) Heredia, K. L.; Tolstyka, Z. P.; Maynard, H. D. Aminooxy End-Functionalized Polymers Synthesized by ATRP for Chemoselective Conjugation to Proteins. *Macromolecules* **2007**, *40* (14), 4772−4779.
(47) Grover, G. N.; Lam, J.; Nguyen, T. H.; Segura, T.; Maynard, H. D. Biocompatible Hydrogels by Oxime Click Chemistry. *Biomacromolecules* **2012**, *13* (10), 3013−3017.
(48) Grover, G. N.; Braden, R. L.; Christman, K. L. Oxime Cross-Linked Injectable Hydrogels for Catheter Delivery. *Adv. Mater.* **2013**, *25* (21), 2937−2942.
(49) Orbán, E.; Mező, G.; Schlage, P.; Csík, G.; Kulić, Ž.; Ansorge, P.; Fellinger, E.; Möller, H.; Manea, M. In Vitro Degradation and Antitumor Activity of Oxime Bond-Linked Daunorubicin−GnRH-III Bioconjugates and DNA-Binding Properties of Daunorubicin−Amino Acid Metabolites. *Amino Acids* **2011**, *41* (2), 469−483.
(50) Jencks, W. P. Studies on the Mechanism of Oxime and Semicarbazone Formation 1. *J. Am. Chem. Soc.* **1959**, *81* (2), 475−481.
(51) Dirksen, A.; Dawson, P. E. Rapid Oxime and Hydrazone Ligations with Aromatic Aldehydes for Biomolecular Labeling. *Bioconjugate Chem.* **2008**, *19* (12), 2543−2548.
(52) Blanden, A. R.; Mukherjee, K.; Dilek, O.; Loew, M.; Bane, S. L. 4-Aminophenylalanine as a Biocompatible Nucleophilic Catalyst for Hydrazone Ligations at Low Temperature and Neutral pH. *Bioconjugate Chem.* **2011**, *22* (10), 1954−1961.
(53) Bryson, D. I.; Zhang, W.; Ray, W. K.; Santos, W. L. Screening of a Branched Peptide Library with HIV-1 TAR RNA. *Mol. BioSyst.* **2009**, *5* (9), 1070−1073.
(54) Bahta, M.; Liu, F.; Kim, S.-E.; Stephen, A. G.; Fisher, R. J.; Burke, T. R. Oxime-Based Linker Libraries As a General Approach for the Rapid Generation and Screening of Multidentate Inhibitors. *Nat. Protocols* **2012**, *7* (4), 686−702.
(55) Moore, J. S.; Stupp, S. I. Room-Temperature Polyesterification. *Macromolecules* **1990**, *23* (1), 65−70.
(56) Lee, M.; Lee, J.-P.; Rhee, H.; Choo, J.; Gyu Chai, Y.; Kyu Lee, E. Applicability of Laser-Induced Raman Microscopy for in Situ Monitoring of Imine Formation in a Glass Microfluidic Chip. *J. Raman Spectrosc.* **2003**, *34* (10), 737−742.
(57) Drury, J. L.; Mooney, D. J. Hydrogels for Tissue Engineering: Scaffold Design Variables and Applications. *Biomaterials* **2003**, *24* (24), 4337−4351.
(58) Gunn, J. W.; Turner, S. D.; Mann, B. K. Adhesive and Mechanical Properties of Hydrogels Influence Neurite Extension. *J. Biomed. Mater. Res., Part A* **2005**, *72A* (1), 91−97.
(59) Marklein, R. A.; Soranno, D. E.; Burdick, J. A. Magnitude and Presentation of Mechanical Signals Influence Adult Stem Cell Behavior in 3-Dimensional Macroporous Hydrogels. *Soft Matter* **2012**, *8* (31), 8113−8120.
(60) Banerjee, A.; Arha, M.; Choudhary, S.; Ashton, R. S.; Bhatia, S. R.; Schaffer, D. V.; Kane, R. S. The Influence of Hydrogel Modulus on the Proliferation and Differentiation of Encapsulated Neural Stem Cells. *Biomaterials* **2009**, *30* (27), 4695−4699.
(61) Ifkovits, J. L.; Tous, E.; Minakawa, M.; Morita, M.; Robb, J. D.; Koomalsingh, K. J.; Gorman, J. H.; Gorman, R. C.; Burdick, J. A. Injectable Hydrogel Properties Influence Infarct Expansion and Extent of Postinfarction Left Ventricular Remodeling in an Ovine Model. *Proc. Natl. Acad. Sci. U.S.A.* **2010**, *107* (25), 11507−11512.
(62) Flory, P. J. Molecular Size Distribution in Three Dimensional Polymers. II. Trifunctional Branching Units. *J. Am. Chem. Soc.* **1941**, *63* (11), 3091−3096.
(63) Stockmayer, W. H. Theory of Molecular Size Distribution and Gel Formation in Branched-Chain Polymers. *J. Chem. Phys.* **1943**, *11* (2), 45−55.

(64) Tibbitt, M. W.; Kloxin, A. M.; Sawicki, L. A.; Anseth, K. S. Mechanical Properties and Degradation of Chain and Step-Polymerized Photodegradable Hydrogels. *Macromolecules* **2013**, *46* (7), 2785−2792.
(65) Sander, E. G.; Jencks, W. P. Equilibria for Additions to the Carbonyl Group. *J. Am. Chem. Soc.* **1968**, *90* (22), 6154−6162.
(66) Byeon, J.-Y.; Limpoco, F. T.; Bailey, R. C. Efficient Bioconjugation of Protein Capture Agents to Biosensor Surfaces Using Aniline-Catalyzed Hydrazone Ligation. *Langmuir* **2010**, *26* (19), 15430−15435.
(67) Tornøe, C. W.; Christensen, C.; Meldal, M. Peptidotriazoles on Solid Phase: [1,2,3]-Triazoles by Regiospecific Copper(I)-Catalyzed 1,3-Dipolar Cycloadditions of Terminal Alkynes to Azides. *J. Org. Chem.* **2002**, *67* (9), 3057−3064.
(68) Gierlich, J.; Burley, G. A.; Gramlich, P. M. E.; Hammond, D. M.; Carell, T. Click Chemistry as a Reliable Method for the High-Density Postsynthetic Functionalization of Alkyne-Modified DNA. *Org. Lett.* **2006**, *8* (17), 3639−3642.
(69) Agard, N. J.; Prescher, J. A.; Bertozzi, C. R.; Strain-Promoted, A. [3 + 2] Azide−Alkyne Cycloaddition for Covalent Modification of Biomolecules in Living Systems. *J. Am. Chem. Soc.* **2004**, *126* (46), 15046−15047.
(70) Baskin, J. M.; Prescher, J. A.; Laughlin, S. T.; Agard, N. J.; Chang, P. V.; Miller, I. A.; Lo, A.; Codelli, J. A.; Bertozzi, C. R. Copper-Free Click Chemistry for Dynamic in Vivo Imaging. *Proc. Natl. Acad. Sci. U.S.A.* **2007**, *104* (43), 16793−16797.
(71) Deng, X.; Friedmann, C.; Lahann, J. Bio-Orthogonal "Double-Click" Chemistry Based on Multifunctional Coatings. *Angew. Chem., Int. Ed.* **2011**, *50* (29), 6522−6526.
(72) Weber, P.; Ohlendorf, D.; Wendoloski, J.; Salemme, F. Structural Origins of High-Affinity Biotin Binding to Streptavidin. *Science* **1989**, *243* (4887), 85−88.
(73) Boekhoven, J.; Poolman, J. M.; Maity, C.; Li, F.; van der Mee, L.; Minkenberg, C. B.; Mendes, E.; van EschJan, H.; Eelkema, R. Catalytic Control over Supramolecular Gel Formation. *Nat. Chem.* **2013**, *5* (5), 433−437.